The Hydrodynamic Resistance, Wave Wakes and Bottom Pressure Signatures of a 5900t Displacement Air Warfare Destroyer

Leo Lazauskas
Dept. Applied Mathematics
The University of Adelaide
South Australia 5005
AUSTRALIA
leo@cyberiad.net

31 July 2007

Abstract

Numerical calculations are performed to predict the calm-water wave resistance, viscous resistance, wave patterns, and bottom pressure signatures of a 5900t displacement ship with the same principal dimensions as the Australian Navy's proposed Hobart Class Air Warfare Destroyer.

Introduction

The purpose of the present note is to estimate the total calm-water hydrodynamic resistance, wave wakes and bottom pressure signatures of a vessel similar to the Australian Navy's Hobart Class operating in deep water and also in Gulf St. Vincent, a relatively shallow body of water in South Australia. The bathymetry of the gulf (taken from [3]) is shown in Figure 2.

Results

Environmental Variables

	Value
g (ms^{-2})	9.80665
Water (15° C)	
ρ (kg/m^3)	1025.87
ν $(10^-6m^2s^{-1})$	1.18831

Table 1: Principal environmental variables.

Table 1 shows the principal environmental variables used to produce the results to follow. Gravitational acceleration is denoted by g; ρ and ν are, respectively, the density and kinematic viscosity of water.

Ship Dimensions

	Values
D (m^3)	5908.0
L_{WL} (m)	134.0
B_{WL} (m)	15.7
T (m)	7.2

Table 2: Principal dimensions and parameters of the (hypothetical) vessel *Nibberluna.*

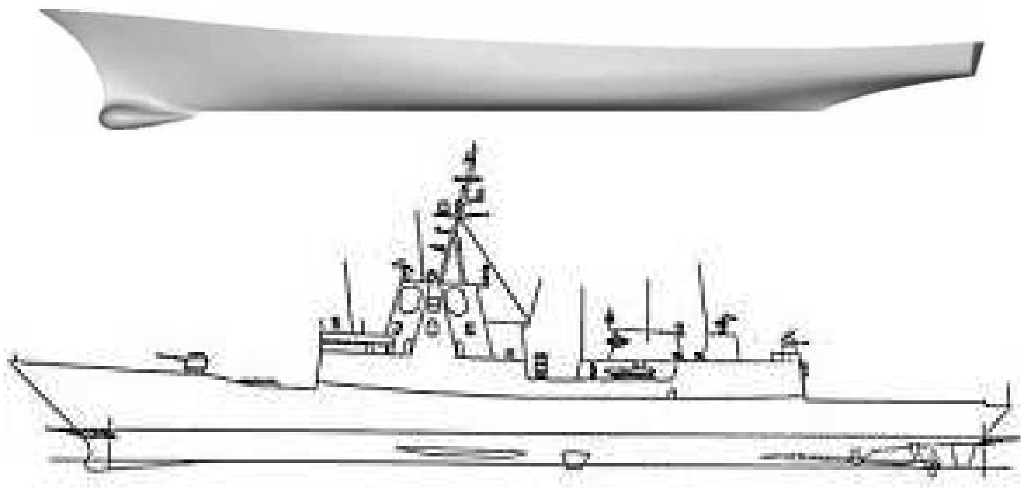

Figure 1: David Taylor Model Basin 5415 hull (top) and F100 (bottom).

The hypothetical vessel used in the present report has been named *Nibberluna*, a Tasmanian Aboriginal name for the region around Hobart and the Derwent River.

The ship has the same (non-dimensional) shape as the DTMB5415 destroyer hull and the principal dimensions of the Hobart Class Air Warfare Destroyer (which in turn is based on the Spanish Navantia F100). Sideviews of the DTMB 5415 hull and the F100 are shown in Figure 1. It can be seen that the underwater portions of the two hulls are quite similar.

The principal underwater dimensions of the *Nibberluna* are given in Table 2. The displacement of the hull is D, its waterline length is L_{WL}, beam B_{WL} and draft T.

Resistance Components

For the purposes of the present report the total hydrodynamic resistance, R_T, is

$$R_T = R_V + R_W + R_H \tag{1}$$

where R_V is the viscous resistance, R_W is the wave resistance and R_H is the transom stern hydrostatic resistance.

In the present report we use Michell's [5] thin-ship integral to estimate the wave resistance. Viscous resistance is estimated using Grigson's [2] skinfriction line which is based on 2D boundary layer theory. Form factors are not used.

We ignore, among other drag components, splash, spray, and wave-breaking, which, in general, comprise a smaller proportion of the total resistance than the other components, particularly for the fine hull we are considering.

The top plot of Figure 3 shows the total resistance and resistance components (in kilo Newtons) in infinitely deep water. It can be seen that wave resistance is the dominant component for the entire speed range of interest.

The bottom plot of Figure 3 shows the effect of water depth on the wave resistance. Depths of 25m and 35m were chosen because they are typical values for Backstairs Passage and Investigator Strait, one of which vessels need to negotiate in order to reach open sea.

It can be seen that depth effects are significant for speeds greater than about 24 knots. At 30 knots in 25m depth, the wave resistance is almost five times that of the deep water value, and three times that of the value in 35m deep water. If the top speed of the vessel is around 30 knots in deep water, then it is very unlikely that it will have sufficient installed power to reach that speed in water depths of 25m or 35m.

Wave Patterns

The method for calculating wave elevations is described in [6] and [7]. A turbulent kinematic eddy viscosity factor of $\nu_t = 0.001 m^2 s^{-1}$ was used with Lamb's [4] wave damping formulation for both speeds. More refined estimates could be made if the actual value of ν_t was known, however it should be noted that ν_t could vary by several orders of magnitude, depending on many poorly understood environmental factors.

The wave field around the vessel travelling at 18 knots and at 28 knots in infinitely deep water is shown in the two plots of Figure 4. The largest wave elevations occur near the bow and the stern of the vessels.

The effect of water depth on far-field wave patterns is shown in Figure 5 for 35m depth and Figure 6 for 25m. Depth effects are not significant for 18 knots, as can be seen by comparing the top plots of the two figures.

At 28 knots, the wave patterns are significantly different from the infinite depth case. In the bottom plot of Figure 5 (where $F_h = 0.78$) the Kelvin angle is slightly larger than its value in infinitely deep water. In 25m depth (where $F_h \approx 0.92$) the Kelvin angle is very wide.

Bottom Pressure Signatures

As well as creating large waves, ships operating in shallow water can also cause damage to the sea bottom, disrupting sea-grass beds and, consequently, the fauna that rely on them. One simple measure of the effect on the sea-bottom is the pressure (above hydrostatic) induced by the passage of water around and underneath the ship hull.

Mine-sweeping is a process for neutralising pressure mines by tricking them into detonating in the absence of an actual ship [1]. It is therefore vitally important to know the bottom pressure signature of the ship so that suitable anti-mine counter-measures can be developed.

Figures 7 and 8 show the bottom pressure (above hydrostatic) on a small patch of seabed underneath the vessel for two depths (35m and 25m) and two different speeds (18 knots and 28 knots). Pressures were calculated using a method based on that described by Tuck [8]. The vessel lies (above the patch) at $y = 0$ and between $x = -67$ and $x = 67$.

At 18 knots in 35m depth, the top plot of Figure 7 shows that bottom pressures vary from a minimum of about -1100Pa below midships, to a maximum of about 400Pa directly below the bow and the stern of the vessel. The depth-based Froude number $F_h = U/\sqrt{(gh)}$ for this case is about 0.5. At 28 knots in the same depth ($F_h \approx 0.78$), the pressure contours are very similar to those at 18 knots, however the pressure variation is about triple that at $F_h = 0.5$, varying from -3700Pa underneath midships to about 1300Pa below the bow and the stern.

The pressure variations for 25m depth are shown in the two plots of Figure 8. Here we see that the pressure contours are similar to each other, but the magnitude of the variations are considerably greater.

At 18 knots in 25m deep water ($F_h \approx 0.59$) pressures vary from a minimum of -2000Pa to a maximum of 800Pa. At 28 knots in the same depth ($F_h \approx 0.92$) the range is -9889Pa to 4068Pa.

It is well beyond the capabilities of the present author to assess whether the magnitude of these (travelling) pressures are significant in terms of seabed disruption.

References

[1] Barnes, John C., "New techniques to predict ship vulnerability to pressure mines along shipping routes", Dept. of Defence, DSTO Report DSTO-RR-0126, Feb. 1998.

[2] Grigson, C.W.B., "A planar friction algorithm and its use in analysing hull resistance", *Trans. RINA*, 2000, pp. 76–115.

[3] Grzechnik, Marcus Paul, "Three-dimensional tide and surge modelling and layered particle tracking techniques applied to South Australian coastal seas", *PhD thesis*, Dept. Applied Mathematics, The University of Adelaide, July 2000.

[4] Lamb, *Hydrodynamics*, 5th Edn., Cambridge, 1932.

[5] Michell, J.H., "The wave resistance of a ship." *Philosophical Magazine*, Series 5, Vol. 45, 1898, pp. 106–123.

[6] Tuck, E.O., Scullen, D.C. and Lazauskas, L., "Sea Wave Pattern Evaluation, Part 6 report: Viscosity factors", The University of Adelaide, Jan. 2002.

[7] Tuck, E.O., Scullen, D.C. and Lazauskas, L., "Ship-wave patterns in the spirit of Michell", *Proceedings of the IUTAM Symposium on Free-Surface Flows*, Birmingham, July 2000, ed. A.C. King and Y.D. Shikhmurzaev, Kluwer Academic Publishers, Dordrecht, 2001, pp. 311–318.

[8] Tuck, E.O., "Bottom Pressure Signatures", Dept. Applied Mathematics, The University of Adelaide, Jan. 1998.

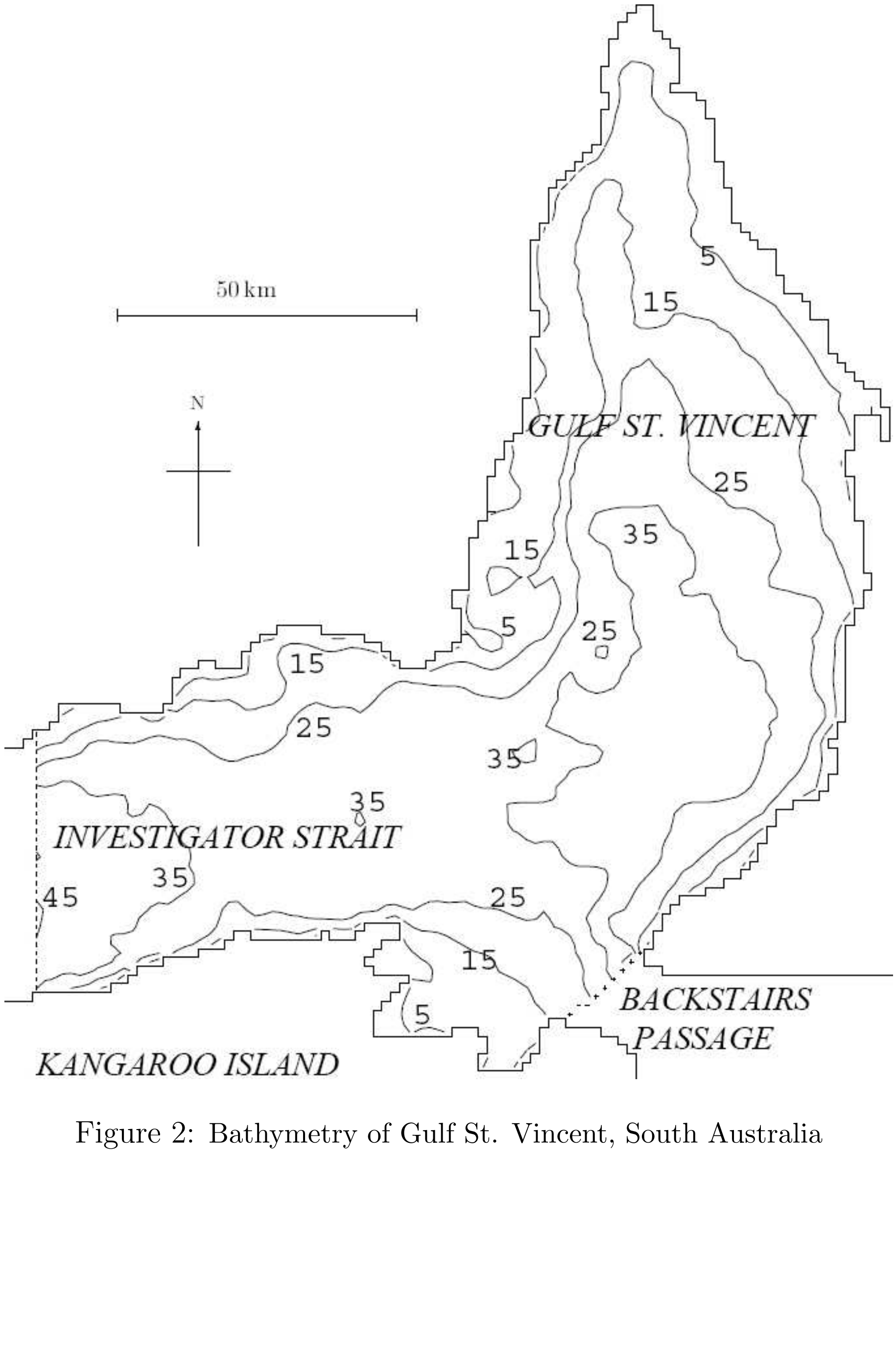

Figure 2: Bathymetry of Gulf St. Vincent, South Australia

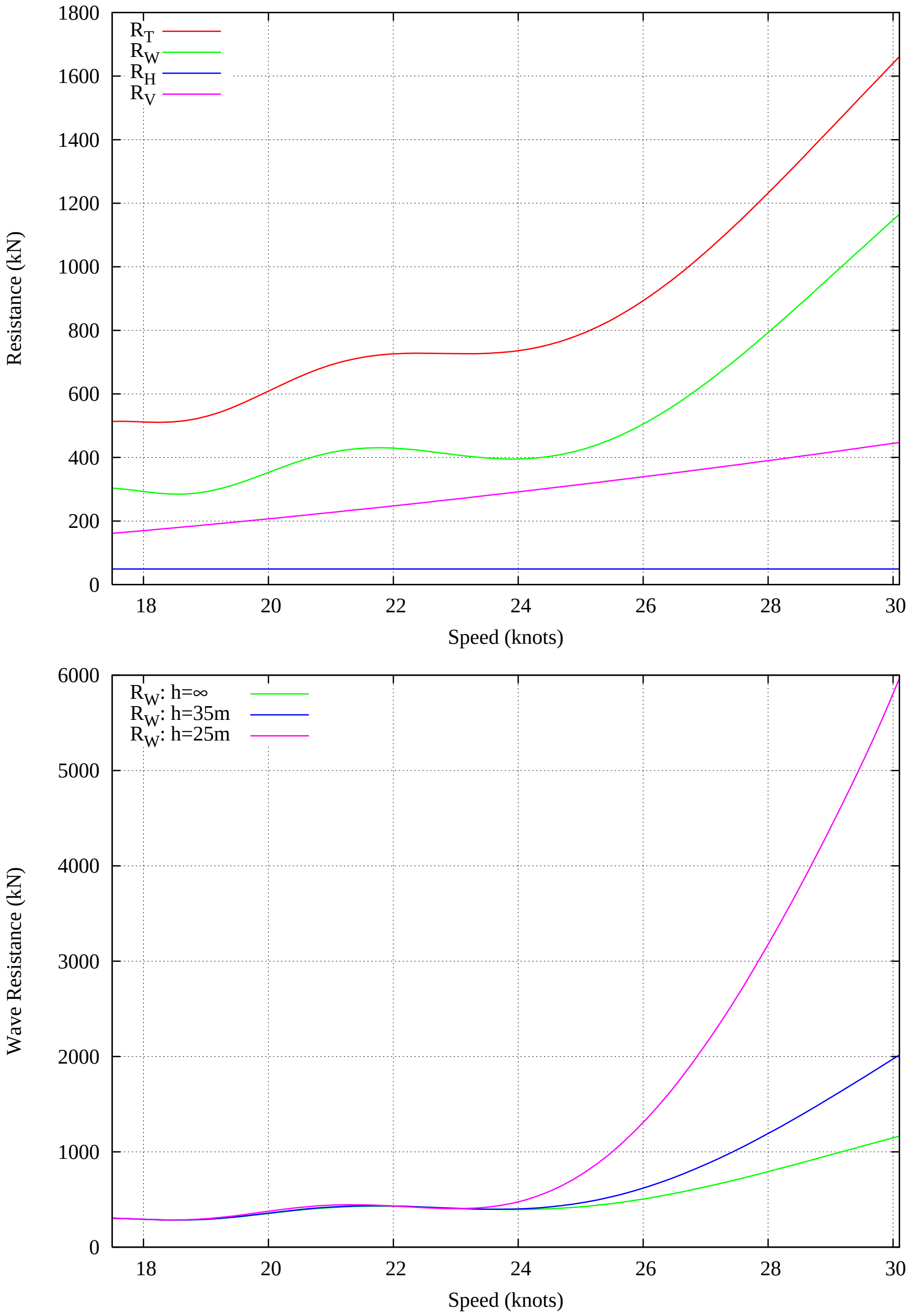

Figure 3: Resistance components in infinitely deep water (top) and wave resistance for different water depths (bottom).

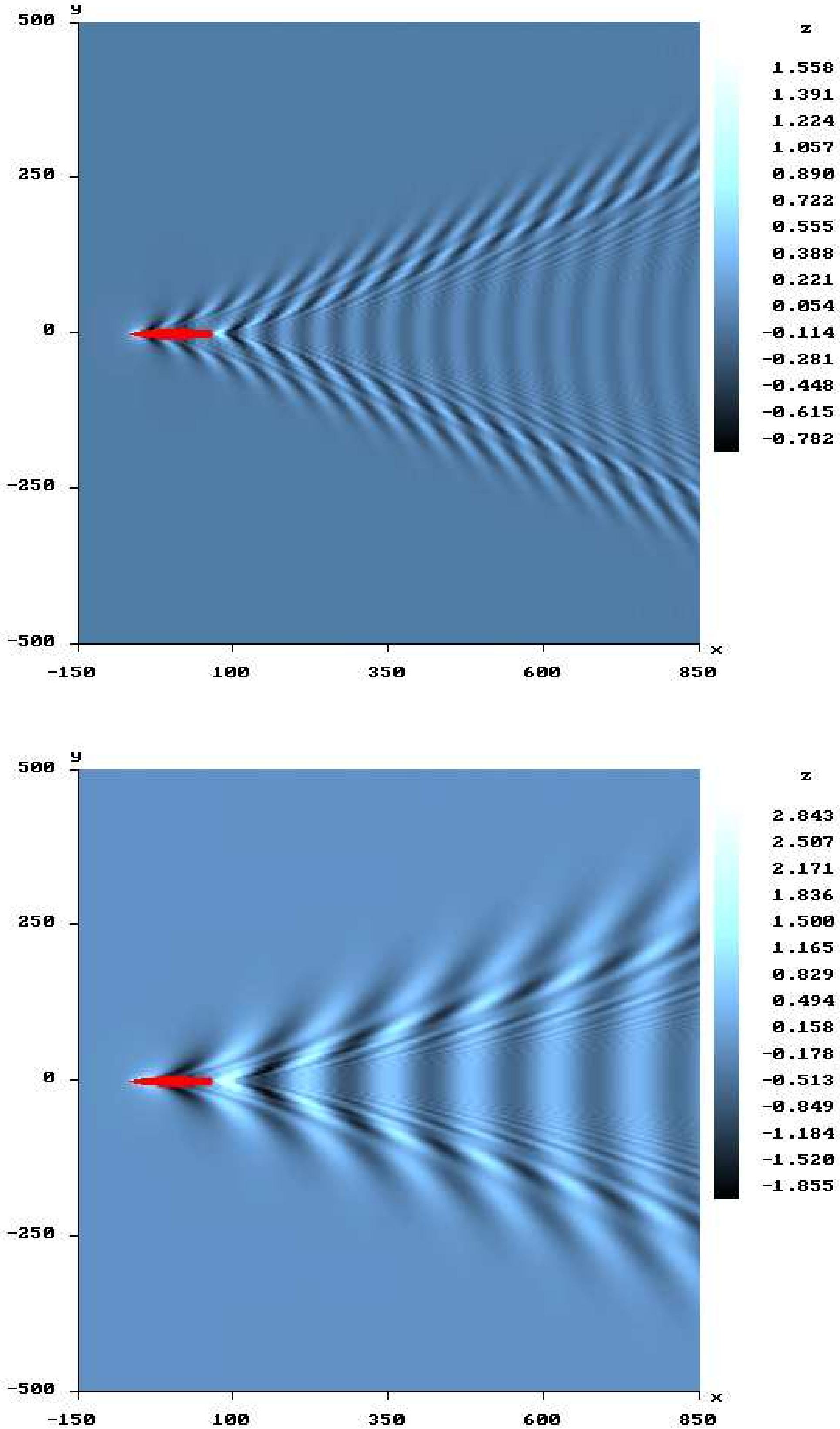

Figure 4: Wave pattern in infinitely deep water at $U = 9.3ms^{-1}$ (top) and $U = 14.4ms^{-1}$ (bottom).

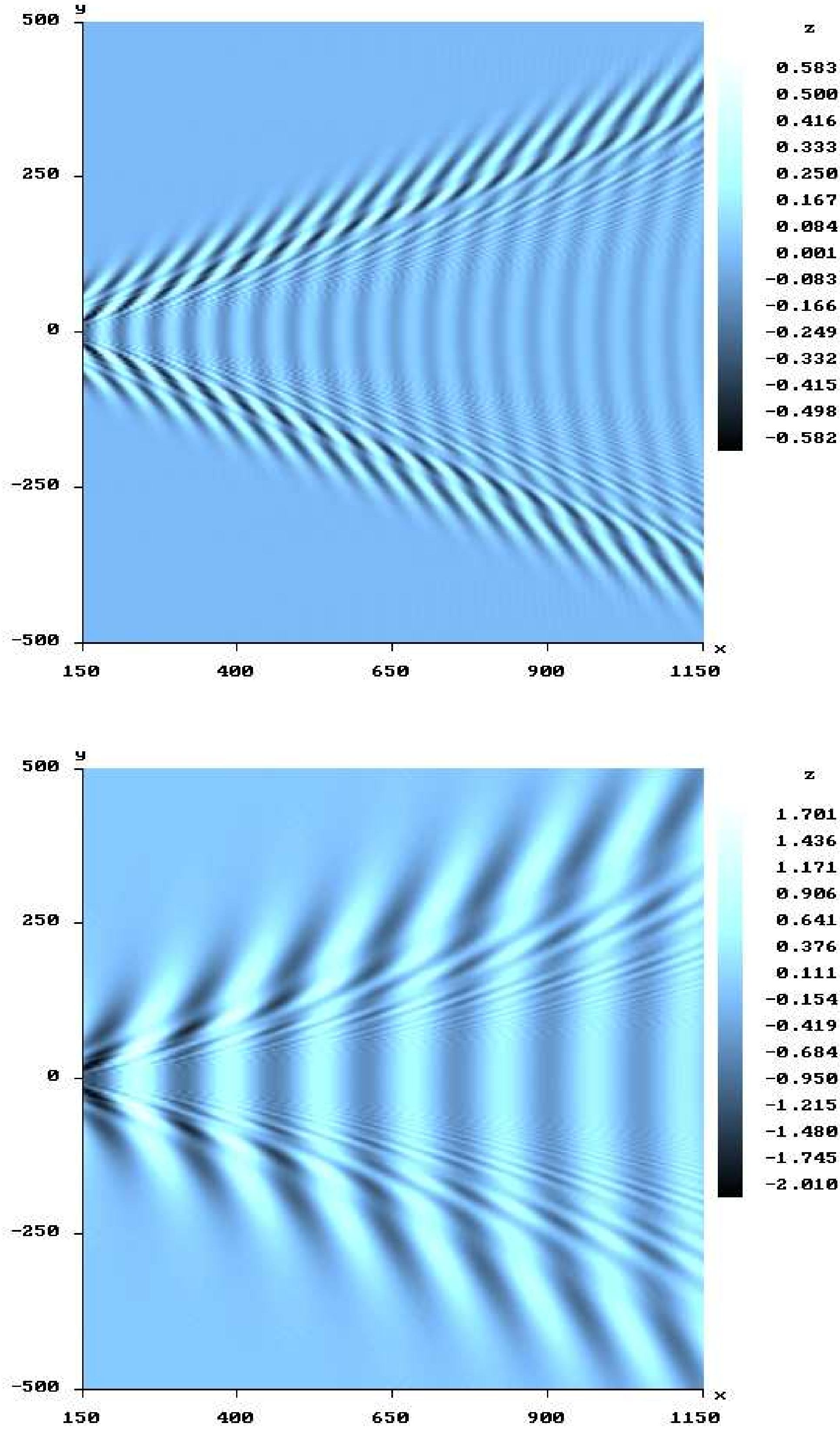

Figure 5: Far-field wave pattern in 35m deep water at $U = 9.3ms^{-1}$ (top) and $U = 14.4ms^{-1}$ (bottom).

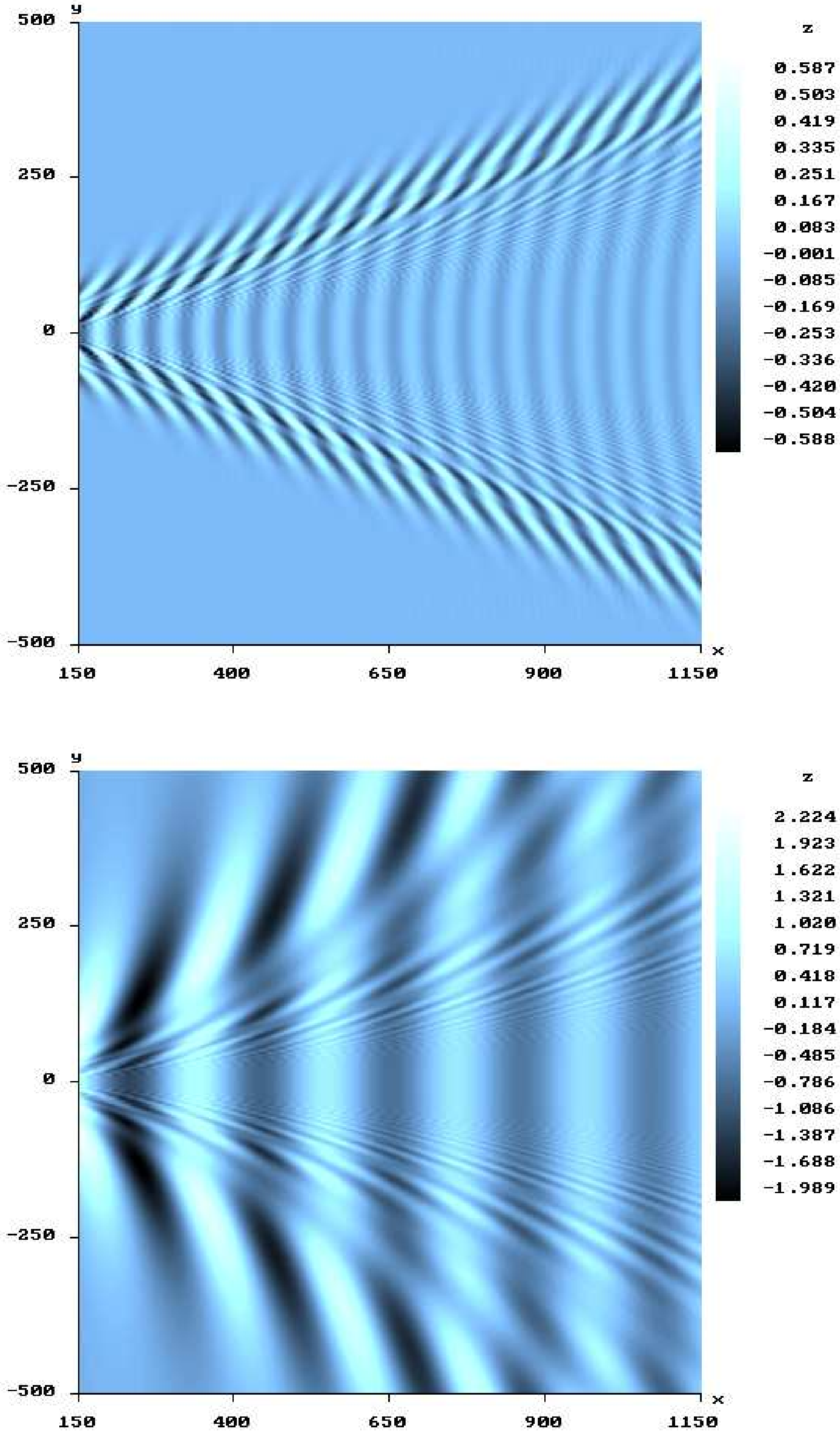

Figure 6: Far-field wave pattern in 25m deep water at $U = 9.3ms^{-1}$ (top) and $U = 14.4ms^{-1}$ (bottom).

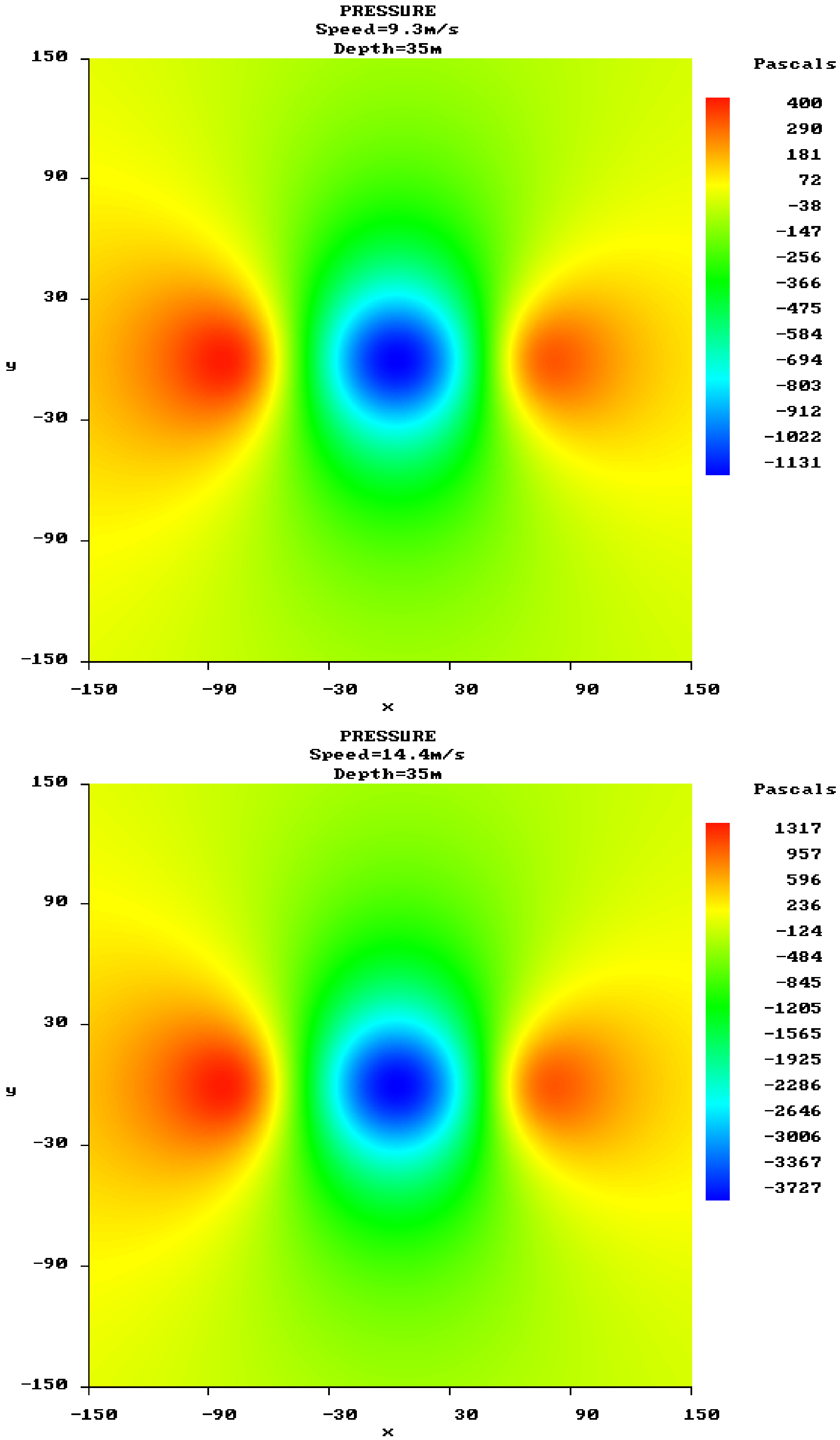

Figure 7: Bottom pressure signatures in 35m deep water: $F_h = 0.50$ (top), $F_h = 0.78$ (bottom)

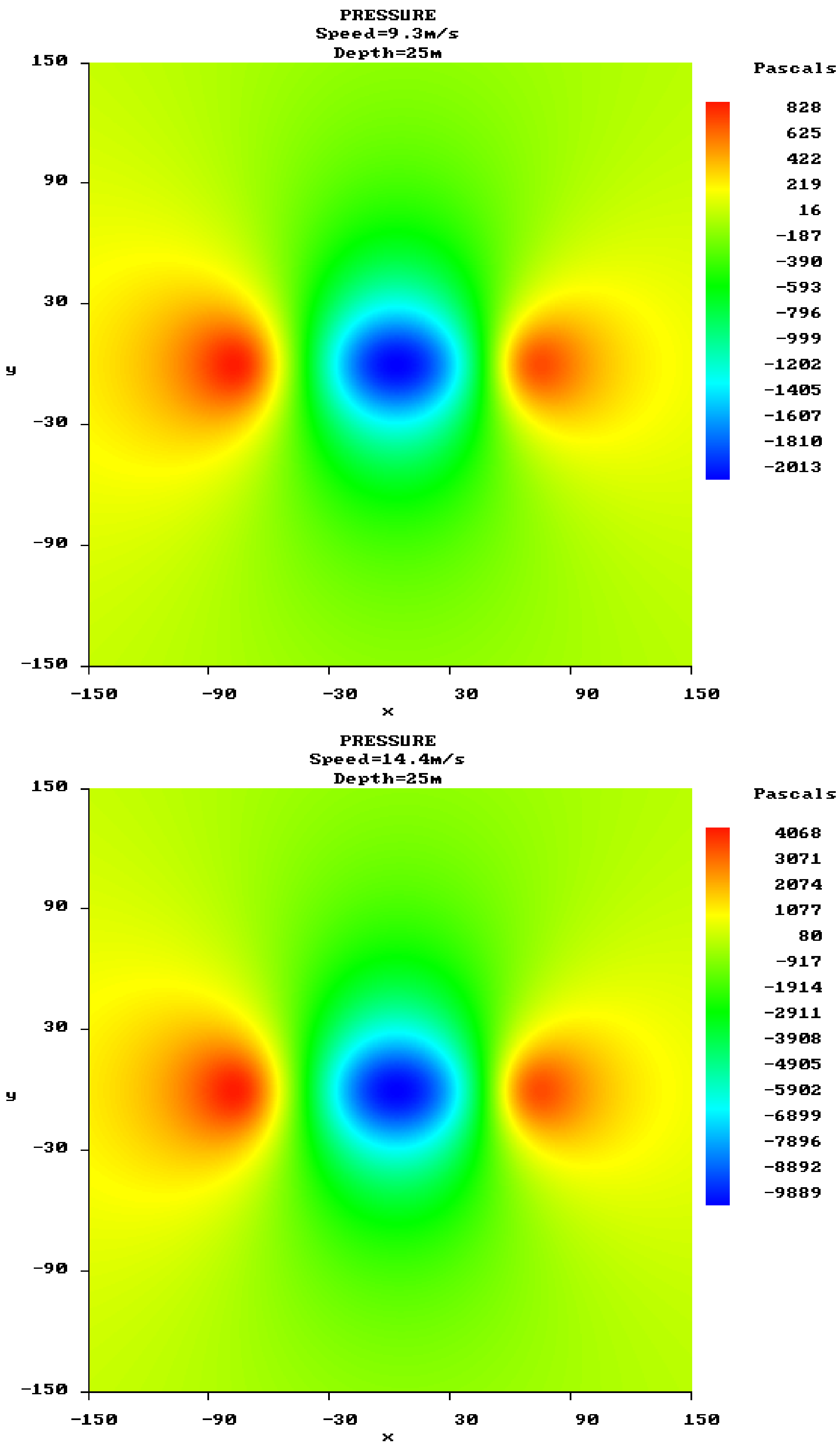

Figure 8: Bottom pressure signatures for 25m deep water: $F_h = 0.59$ (top), $F_h = 0.92$ (bottom)